Figures and Tables

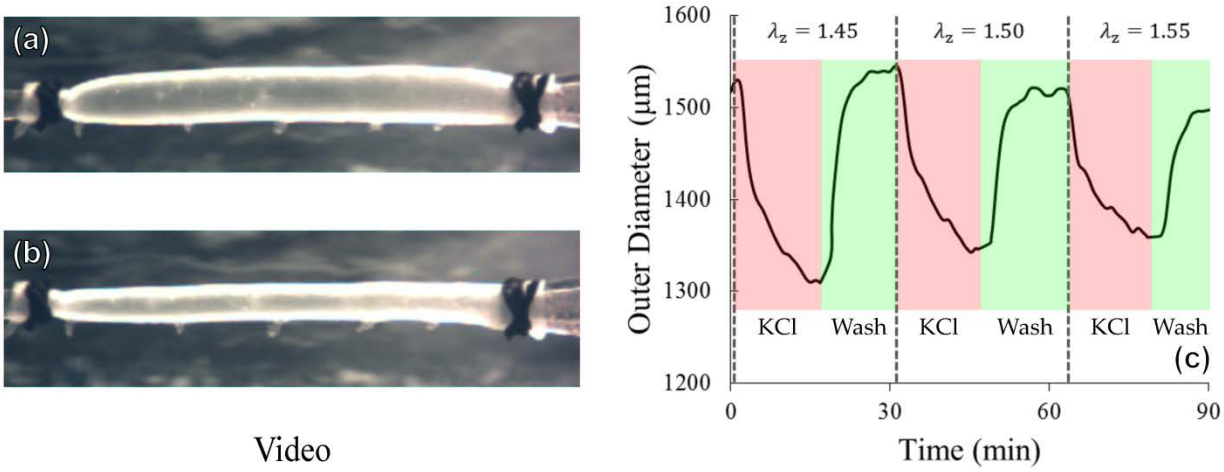

Figure I. Protocol for active biaxial testing. Video-images (left) of a representative cannulated descending thoracic aorta (DTA), within the biaxial testing device, both (a) before and (b) 15 minutes after SMC stimulation with high K^+ while maintained at a 70 mmHg luminal pressure and near the in vivo axial stretch. Actual time course (right) of respective changes in outer diameter (along the ordinate), where contractions via 80 mM KCl are highlighted in pink and relaxations via wash-out with a standard Krebs solution are highlighted in green; the three sections show contraction-relaxation at three different axial stretches. This protocol was repeated for each specimen at 3 different pressures, hence resulting in 9 different contractile states. See Figure VII below. Note, too, the ligated intercostal arteries in the video images; based on visual observations in DTAs and the lack of delaminations in the ascending thoracic aortas (ATAs), which did not have branches within the region of testing, the intercostal branches may have served to help nucleate the in vitro delaminations discussed below.

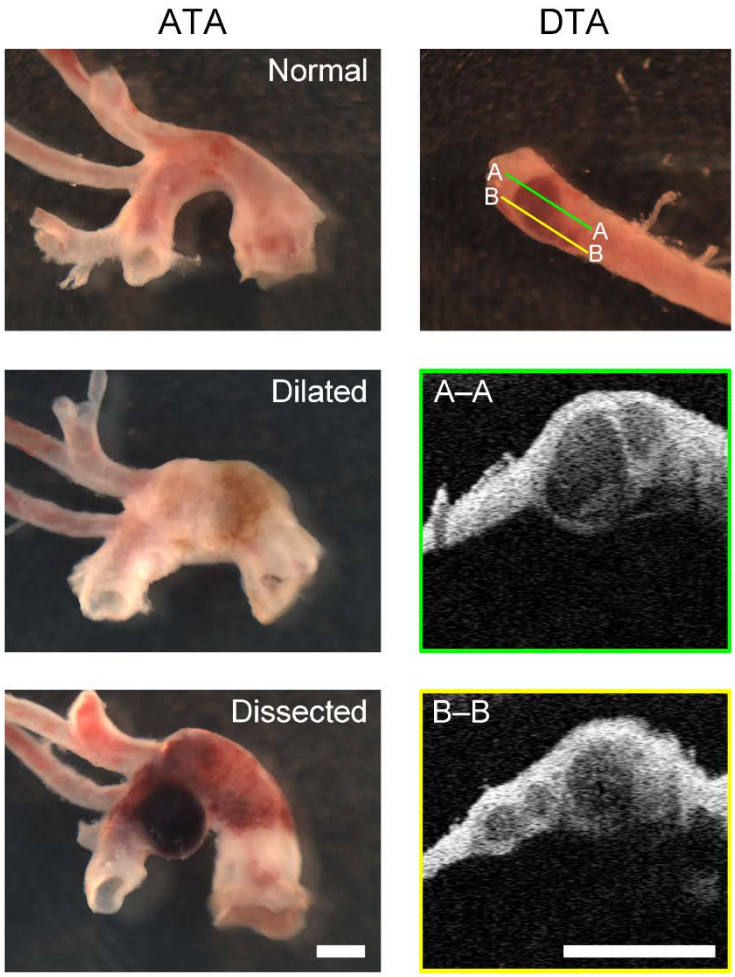

Figure II. Gross phenotypes of three representative ascending thoracic aortas (ATAs) and one descending thoracic aorta (DTA) after 4 weeks of *Tgfbr2* disruption (Tmx). ATAs (left panels) showed diverse phenotypes ranging from normal (top-left) to dilated and fibrotic (middle-left) or dramatic dissection, which is revealed by intramural blood (bottom-left). Note that phenotypic abnormalities involved the ascending and the arch regions while leaving the aortic root mostly unaffected. In contrast, the DTA (right panels) showed a milder phenotype with normal unloaded dimensions. DTA dissections manifested primarily as blood pools localized immediately after the left subclavian branch (top - right). Optical coherence tomography, or OCT, images of the intramural hematomas (middle- and bottom-right) never revealed an intimal flap, but rather multiple apparently separate intramural hematomas that often contributed to the formation of the main dissection. Finally, despite these different manifestations, the percentage of lesions was only slightly higher in the ATA than in the DTA, with an overall dissection rate in vivo about 42%. The white scale bars represent 1 mm.

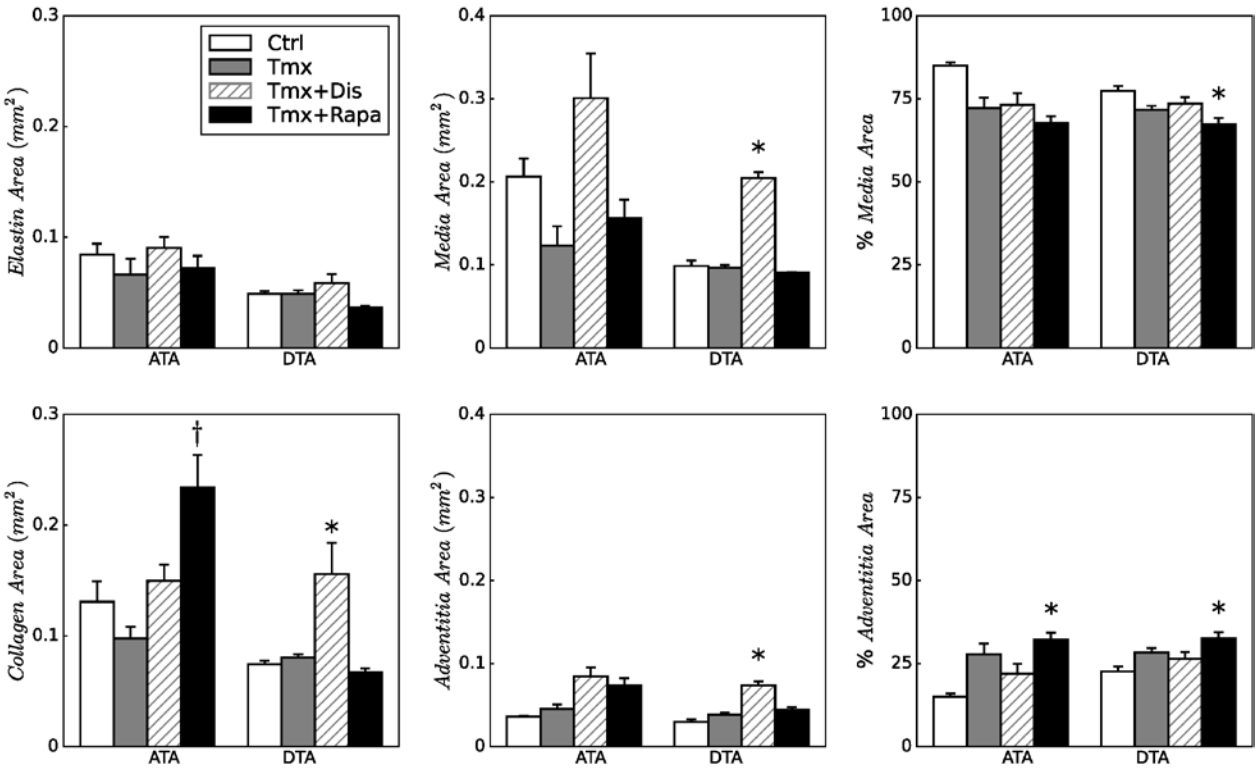

Figure III. Quantification of the microstructural composition (left panels) and layer organization (middle and right panels) in thoracic aortas after *Tgfbr2* disruption. ATA is ascending thoracic aorta whereas DTA is descending thoracic aorta. Elastin areas measured from VVG images did not show any significant differences among the four experimental groups (Ctrl, Tmx, Tmx + Dis, Tmx + Rapa), but did confirm that the elastin content is higher in the ATA than the DTA. Collagen areas were measured from MTC-stained cross sections, thus accounting for total collagen content, which was significantly higher in Tmx + Dis DTAs and Tmx + Rapa ATAs (with respect to Tmx). Medial and adventitial areas were measured from MOV images and showed a clear thickening of both layers in dissected DTAs, with similar – albeit not significant – trends in ATAs. Despite the smaller size of Tmx + Rapa DTAs (Table S2), which correlated well with the smaller body mass of the animals (Table 1), such vessels displayed a moderate increase in adventitial area ($p < 0.1$) while maintaining medial area unchanged. Similar trends were seen in Tmx + Rapa ATAs without reaching statistical significance. Differences in total aortic areas can be due to treatment or aortic location, thus we calculated the percent aortic cross section that is occupied by media and adventitia. Daily treatment with rapamycin following *Tgfbr2* disruption led to an increased percentage of adventitial area in both ATAs and DTAs due to adventitial thickening. The * and † indicate, respectively, $p < 0.05$ compared with Ctrl and Tmx samples from similar aortic locations.

Figure IV. Estimation of the stress-free configuration via the introduction of a radial cut in ascending thoracic aortas (ATA – top row) and descending thoracic aortas (DTA – bottom row) for all three primary groups: controls (Ctrl – first column), tamoxifen-induced disruption of *Tgfbr2* without dissection (Tmx – second column), and tamoxifen-induced disruption with daily treatment with rapamycin (Tmx + Rapa – third column). Residual strains are reflected by the opening angle Φ_0 (bar plot – fourth column). *Tgfbr2* disruption associated with a marked decrease in opening angles in ATAs, with no significant protection or improvement with rapamycin treatment. Similar trends were observed in DTAs despite the lack of statistical significance. Larger opening angles reflect the presence of larger residual stresses (i.e., greater compressive stresses in the inner wall and greater tensile stresses in the outer wall, both in unloaded but intact specimens). The scale bar represents 1 mm. * indicates $p < 0.05$ with respect to Ctrl samples from similar aortic locations.

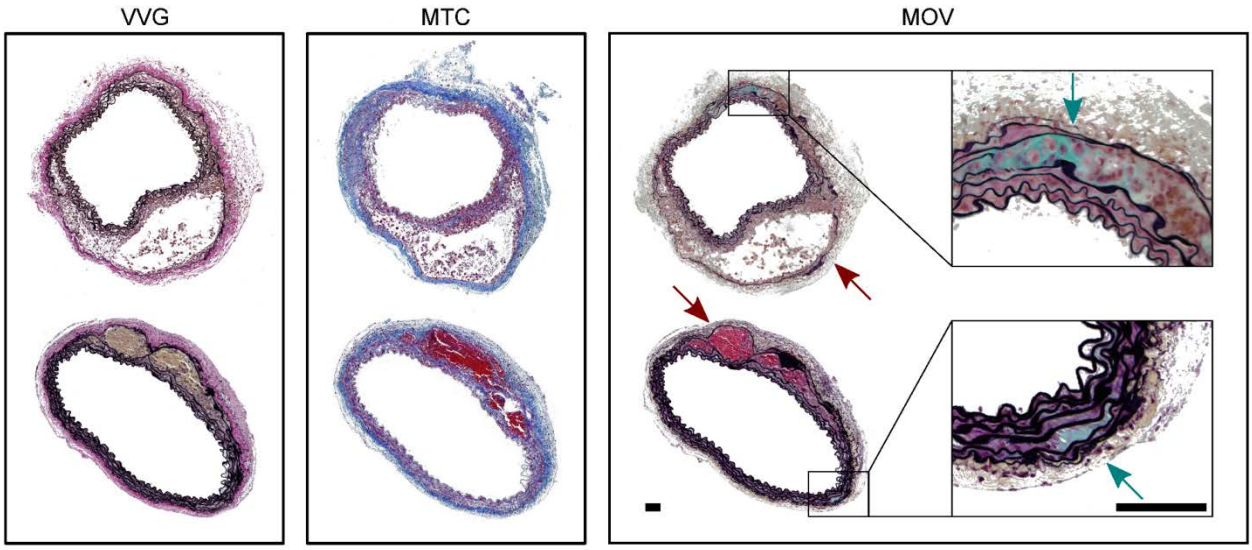

Figure V. Cross-sectional views of DTAs that dissected in vivo and were stained with Verhoeff Van Gieson (VVG - left), Masson's trichrome (MTC - center), or Movat's pentachrome (MOV - right). These images summarize the main pathological phenotypes occurring with dissection after tamoxifen-induced, postnatal disruption of *Tgfbr2*. The red arrows indicate dramatic intramural hematomas (red in MTC and MOV) contained within multiple elastic laminae (black in VVG and MOV sections). The aqua arrows instead highlight localized accumulations of mucoid material (aqua / green in the MOV sections), likely glycosaminoglycans. The mucoid pools often manifested distant from the dissected region, but were nevertheless often within the same intramural layers in which the dissections occurred. Albeit not shown, rapamycin treatment tended to prevent the pooling of mucoid material even though it did not reduce the overall amount. Insets show magnified views of the aortic wall. The scale bars represent 200 μm.

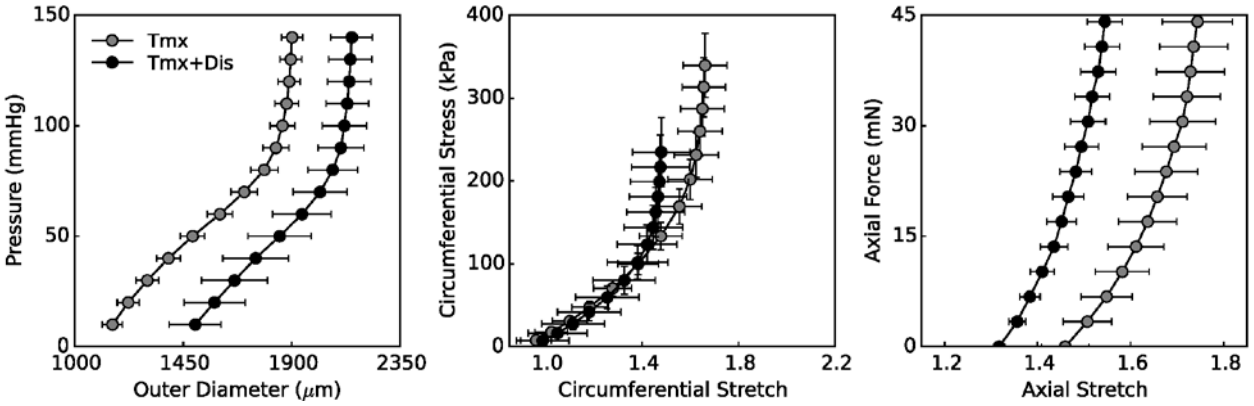

Figure VI. Passive biaxial mechanical behaviors from ascending thoracic aortas (ATA) comparing two subgroups of tamoxifen-induced disruption of *Tgfbr2*: specimens without dissection (Tmx) and specimens that experienced aortic dissection in vivo with an accumulation of blood within the media (Tmx + Dis). Dissection associated with circumferential dilation of the ATA wall (*P-d* data – first column), loss of distensibility shown as a leftward shift in the associated circumferential Cauchy stress-stretch data for cyclic *P-d* tests (second column), and loss of extensibility (*f-l* data – third column). Such changes were not seen in dissected DTA samples (not shown) due to the localized proximal nature of their dissections and the measurement of mechanical quantities away from the lesions (Figure II).

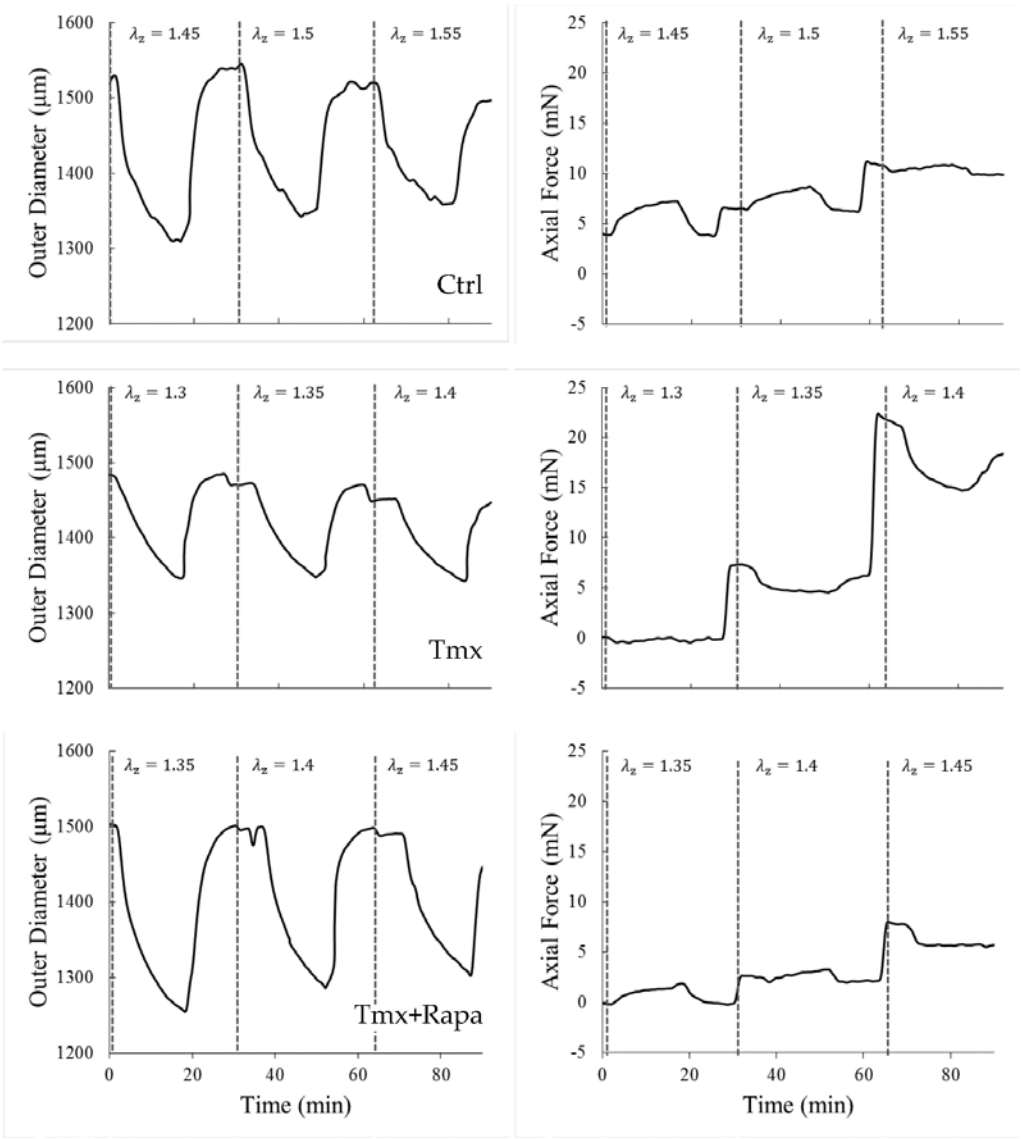

Figure VII. Representative active biaxial data for all three groups: controls (Ctrl – top row), tamoxifen-induced disruption of *Tgfbr2* without dissection (Tmx – middle row), and tamoxifen-induced disruption with daily treatment with rapamycin (Tmx + Rapa – bottom row). Changes in outer diameter over time (left column) indicate that smaller contractions are obtained for higher axial stretches (around the in vivo condition), whereas changes in axial force over time (right column) show that for each vessel there exists a value of axial stretch (called the active in vivo axial stretch) for which measured axial force does not change much upon SMC stimulation. Albeit not shown here, isochoric changes in wall thickness during contraction appeared to reflect differences in "active and passive" in vivo axial stretches. When the active in vivo axial stretch is less than the passive value, the vessel will expand axially during contraction (negative change in axial force), as observed in *Tgfbr2* disrupted DTAs which exhibit a small active increase in wall thickness. Conversely, when the active in vivo axial stretch is greater than the passive value, the vessel will retract axially during contraction (positive change in axial force), as observed in rapamycin treated DTAs which exhibit larger active increases in wall thickness. Increased wall thickness reduces wall stress, which should be protective.

Table I

	ATA			DTA		
	Ctrl	**Tmx**	**Tmx + Rapa**	**Ctrl**	**Tmx**	**Tmx + Rapa**
n	7	6	6	7	7	6
Unloaded and Stress-Free						
Outer Diameter (μm)	1071 ± 27	1249 ± 52*	1076 ± 46	921 ± 18	931 ± 32	822 ± 13*†
Wall Thickness (μm)	106 ± 3	134 ± 9*	120 ± 6	105 ± 4	108 ± 3	117 ± 2
In-vitro Axial Length (mm)	2.8 ± 0.1	2.6 ± 0.1	2.5 ± 0.1	5.0 ± 0.3	5.1 ± 0.3	5.8 ± 0.5
Opening Angle (deg)	74 ± 8	8 ± 4*	17 ± 3*	43 ± 8	17 ± 11	11 ± 5
Loaded at 100 mmHg						
Outer Diameter (μm)	1778 ± 17	1802 ± 45	1590 ± 35*†	1532 ± 37	1497 ± 54	1280 ± 17*†
Wall Thickness (μm)	34 ± 2	53 ± 8*	46 ± 4	38 ± 1	44 ± 1*	50 ± 1*†
In-vivo Axial Stretch	1.74 ± 0.04	1.69 ± 0.08	1.63 ± 0.03	1.50 ± 0.01	1.40 ± 0.03*	1.34 ± 0.01*
Cauchy Stresses (kPa)						
Circumferential	344.2 ± 23.4	240.8 ± 38.5	226.5 ± 20.1*	255.7 ± 8.4	217.6 ± 14.6*	157.3 ± 3.1*†
Axial	355.0 ± 25.9	220.3 ± 45.1*	254.6 ± 28.7	211.0 ± 11.5	157.4 ± 13.5*	125.8 ± 8.4*
Material Stiffness (MPa)						
Circumferential	1.68 ± 0.13	1.56 ± 0.15	1.31 ± 0.10	1.52 ± 0.10	1.71 ± 0.19	1.09 ± 0.06†
Axial	2.15 ± 0.17	1.42 ± 0.34	1.53 ± 0.21	2.47 ± 0.12	2.03 ± 0.14	2.01 ± 0.24
Stored Energy (kPa)	104.3 ± 10.2	59.7 ± 14.5*	66.2 ± 8.7	67.1 ± 2.3	46.7 ± 5.4*	34.1 ± 1.8*
Energy Dissipation Ratio (%)	2.57 ± 0.50	5.70 ± 0.44*	3.71 ± 0.31†	3.26 ± 0.43	4.62 ± 0.81	2.74 ± 0.36

*$p<0.05$ with respect to Ctrl

†$p<0.05$ with respect to Tmx

Table I. Morphological and passive mechanical metrics for ascending thoracic aortas (ATA) and descending thoracic aortas (DTA) for all three primary groups: controls (Ctrl), tamoxifen-induced disruption of *Tgfbr2* (Tmx), and tamoxifen-induced disruption with daily treatment with rapamycin (Tmx+Rapa). The mechanical metrics were evaluated at the group specific in vivo values of axial stretch but a common distending (transmural) pressure of 100 mmHg. Note, therefore, that mean (luminal) arterial pressures, measured using an invasive central catheter under anesthesia, were 84.3±4.3, 77.4±3.1, and 77.6±3.3 mmHg, respectively. Consistent with Figures 2 and 3 in the main paper, *Tgfbr2* disruption resulted in lower energy storage and biaxial stresses but little difference in material stiffness. Rapamycin neither preserved nor restored passive wall properties. On the other hand, *Tgfbr2* disruption caused an increase in energy dissipation in the ATA that was maintained at or brought towards normal values with rapamycin treatment. The same trends were observed in the DTA, despite lacking statistical significance. The * and † indicate, respectively, $p < 0.05$ compared to Ctrl and Tmx samples from similar aortic locations. Data are shown only for vessels that did not delaminate prior to data collection.

Table II

		Circumferential Stress (kPa)			Axial Stress (kPa)		
		Relaxed	Contracted	Change	Relaxed	Contracted	Change
P = 70 mmHg	Ctrl	127 ± 11	75 ± 7	52 ± 5	142 ± 11	119 ± 8	23 ± 3
	Tmx	96 ± 8	70 ± 9	26 ± 4*	58 ± 5*	48 ± 5*	10 ± 1*
	Tmx + Rapa	95 ± 2*	56 ± 5	39 ± 3	67 ± 10*	51 ± 10*	16 ± 1
P = 80 mmHg	Ctrl	187 ± 14	149 ± 12	38 ± 2	128 ± 10	116 ± 10	12 ± 0.5
	Tmx	121 ± 11*	103 ± 14*	19 ± 3*	59 ± 8*	47 ± 7*	11 ± 2
	Tmx + Rapa	120 ± 3*	85 ± 6*	35 ± 3	68 ± 7*	53 ± 7*	15 ± 2
P = 90 mmHg	Ctrl	216 ± 20	206 ± 17	10 ± 7	141 ± 11	130 ± 10	11 ± 4
	Tmx	144 ± 13*	140 ± 14*	4 ± 2	59 ± 9*	55 ± 10*	5 ± 1
	Tmx + Rapa	143 ± 5*	127 ± 9*	16 ± 6	71 ± 5*	59 ± 6*	12 ± 4

*p<0.05 with respect to Ctrl

Table II. Mean wall stresses during active and passive biaxial testing in descending thoracic aortas (DTA) for all three groups: controls (Ctrl), tamoxifen-induced disruption of *Tgfbr2* (Tmx), and tamoxifen-induced disruption with daily treatment with rapamycin (Tmx+Rapa). Biaxial stresses were evaluated from raw data by enforcing equilibrium at the three levels of intraluminal pressure (70, 80, and 90 mmHg) and individual estimated value of in vivo axial stretch. SMC contraction reduces both circumferential (expected from Laplace's equation due to the reduced radius and increased wall thickness) and axial stress. While both relaxed (passive) and contracted (active) stresses are influenced by long-term remodeling of the aortic wall, the displayed change in biaxial stress here (relaxed minus contracted) is due to acute contractility of intramural SMCs. *Tgfbr2* disrupted DTAs display consistently lower changes in stress when stimulated with high KCl due to a reduced contractile capacity, whereas treatment with rapamycin either preserved or restored nearly to normal the values of wall stress. Together with the observation of in vitro delaminations under passive conditions (Figures 5 and 6 in the main text), these data suggest that normal SMC contractility can protect an otherwise vulnerable aortic wall. * indicates $p < 0.05$ with respect to Ctrl samples from similar aortic locations.